Analytical solutions for the short-term plasticity

Paulo R. Protachevicz [a,b,*], Antonio M. Batista [a,c], Iberê L. Caldas [a], Murilo S. Baptista [b]

[a] *Physics Institute, University of São Paulo, São Paulo, SP, Brazil*
[b] *Institute for Complex Systems and Mathematical Biology, Department of Physics, SUPA, University of Aberdeen, Aberdeen, United Kingdom*
[c] *Mathematics and Statistics Department, State University of Ponta Grossa, Ponta Grossa, PR, Brazil*

ARTICLE INFO

ABSTRACT

Synaptic dynamics plays a key role in neuronal communication. Due to its high dimensionality, the main fundamental mechanisms triggering different synaptic dynamics and their relation with the neurotransmitter release regimes (facilitation, biphasic, and depression) are still elusive. For a general set of parameters, and employing an approximated solution for a set of differential equations associated with a synaptic model, we obtain a discrete map that provides analytical solutions that shed light on the dynamics of synapses. Assuming that the presynaptic neuron perturbing the neuron whose synapse is being modelled is spiking periodically, we derive the stable equilibria and the maximal values for the release regimes as a function of the percentage of neurotransmitter released and the mean frequency of the presynaptic spiking neuron. Assuming that the presynaptic neuron is spiking stochastically following a Poisson distribution, we demonstrate that the equations for the time average of the trajectory are the same as the map under the periodic presynaptic stimulus, admitting the same equilibrium points. Thus, the synapses under stochastic presynaptic spikes, emulating the spiking behaviour produced by a complex neural network, wander around the equilibrium points of the synapses under periodic stimulus, which can be fully analytically calculated.

1. Introduction

Synapses are specialized structures in neuronal communication which play a key role in the transmission of neuronal signals in the brain [1]. There are two types of synapses, the electrical and the chemical [2]. Through the electrical synapses, neurons communicate with each other by direct exchange of ion currents [3]. In the axon terminals of the presynaptic neurons with chemical synapses, the action potentials generate the release of neurotransmitters in the synaptic cleft that arrive at the receptors and then produce a current in the postsynaptic neurons [4]. In the mammalian brain, most synapses are chemical [5]. The effectiveness of these transmitted currents depends on the synaptic strength that usually changes in time due to the previous activity of the synapse [6].

Some mathematical models were proposed in the literature to describe the dynamics of chemical synapses. Many of them provide a simplified description of the signal transmission between the neurons [7], for instance, single exponential decay, alpha, and double exponential synaptic functions [8,9]. However, in these models, the maximal conductance associated with each spike event has a fixed value and does not exhibit synaptic regimes, such as facilitation and

depression [10]. Others, however, provide more realistic synaptic dynamics where the intensity of synaptic conductance is altered over time [11]. This process of change in the synaptic intensity is called synaptic plasticity [12], where short- and long-term are the two main types of synaptic plasticity [13]. While for a long time scale, plasticity can exhibit long-term potentiation (LTP) or depression (LTD) [14,15], for short time scales, the synaptic dynamics are associated with facilitation, depression and biphasic regimes [16–18]. Both facilitation and depression synaptic regimes are found between excitatory neurons in the neocortex [19]. These two kinds of plasticity also have different functions in the brain, for example, long-term plasticity is associated with processes such as memory and learning, while short-term plasticity is related to processing functions and working memory in neural circuits [20,21].

In simple terms, short-term plasticity consists of the changes in synaptic strength conductance in a relatively small period of time which are associated with the release of neurotransmitters in each synapse [22]. These synaptic changes can act in the time scale of milliseconds to seconds, but can also last longer in the order of minutes [23–25]. A relevant model in this framework for short-term plasticity was introduced by Markram et al. [26]. According to it, spiking

frequency and the amount of neurotransmitters released in the synaptic cleft are two important factors in synaptic dynamics [22]. The mechanism described by the mentioned model considers that the changes in synaptic transmission strengths depend mainly on the spike activity of the presynaptic neuron [27]. Depending on the time constants, frequency of spikes, and the amount of neurotransmitter released, different regimes such as facilitation, depression, and biphasic regime of the synapse can emerge [28]. The synapses with a high probability of release tend to present short-term depression [29]. On the other hand, facilitation regimes emerge when the number of vesicles available increases due to consecutive spikes [30]. In addition, the combination of depression and facilitation has been reported to generate particular synaptic and network dynamics [31,32].

An important behaviour found in neuron activities is the spike variability [7]. To study neuronal activities, Poisson processes are standard to model the spike time variability of irregular firings [33–35]. The Poisson process can be considered as homogeneous [36] or inhomogeneous [37]. The main difference between these two types of Poisson processes is that the homogeneous has a constant rate of events over time while the inhomogeneous has the rate of events changing over time [38,39]. In the field of neuroscience, the Poisson process is considered as an approximation for spontaneous neuron spikes that can be useful to investigate some aspects of neuronal dynamics [40–42]. Moreover, the Poisson process is one of the simple ways to describe the spike activities with stochastic firings [43]. There are some evidences that Poisson-like behaviours can be related to the emergence of neuronal variability [44]. The Poisson distribution allows us to derive results which, under certain conditions, are relate to real dynamics. Neurons can exhibit near periodic and Poissonian spike activities over time [45]. The comprehension of how periodic and Poisson-like spike activities induce different synaptic dynamics can shed light into the understanding of neuronal communication.

In this work, we obtain a map from a synaptic model described by a set of fourth ODEs proposed by Tsodyks et al. [22], and analyse how different synaptic states depend on relevant parameters, such as the spiking frequency of presynaptic neuron and the percentage of neurotransmitters released. We obtain analytically the equilibrium points in the periodic regime, identify the synaptic regimes, and determine the final and maximal value of active neurotransmitters in the space parameter of frequency and the fraction of neurotransmitters released. The maximal value corresponds to the most intense release of neurotransmitters that can generate the highest synaptic currents on the postsynaptic neurons. However, the interest in analytically calculating these values is because the solution will depend on the peculiarities of the transient behaviour in biphasic and depression, and the asymptotic behaviour of the facilitation. Furthermore, we identify when the maximal fraction of active neurotransmitters can occur in each regime. In addition to that, assuming that the presynaptic neuron is spiking following a Poisson distribution, we showed that the equations for the time average of the trajectory are the same as the map under periodic presynaptic stimulus, admitting the same equilibrium points. The periodic and Poisson spikes are approximations of the dynamics observed in real neuronal dynamics for regular and random spikes. Furthermore, we demonstrate numerically the correctness of our analytical derivations for the map and its equilibrium points of active neurotransmitters. These results can contribute to understand how communication in the brain is mediated by synapses under regular or irregular stimulus.

The paper is organized as follows. In Section 2, we introduced the synaptic model considered in this work. In Section 3, we showed the analytical and numerical results. In the last section, we draw our conclusions.

2. Methods

In short-term plasticity, the effective synaptic conductance changes in time depending on the neuron spike historic. The relevant parameters in synaptic dynamics are the presynaptic neuron firing frequency, the percentage of neurotransmitters released, and the time constants of the synapse. All these parameters in the model take into account the fact that there is a finite amount of neurotransmitters in each synapse and that they are not always available in the same quantity over time. Based on this, to study the synaptic dynamics, we considered the phenomenological model proposed in [22]. The model considered in this study is based on a map derived to describe experimental data reported in [46], which was modelled by an ODE in [22]. We provide a map and solutions for the ODE system proposed in [22].

In this model, each directional synaptic connection from a presynaptic neuron [47] is represented by the set of ODEs

$$\frac{dx}{dt} = \frac{z}{\tau_{\text{rec}}} - xu\delta(t - t^{\text{sp}}), \tag{1}$$

$$\frac{dy}{dt} = -\frac{y}{\tau_{\text{ina}}} + xu\delta(t - t^{\text{sp}}), \tag{2}$$

$$\frac{dz}{dt} = \frac{y}{\tau_{\text{ina}}} - \frac{z}{\tau_{\text{rec}}}, \tag{3}$$

$$\frac{du}{dt} = -\frac{u}{\tau_{\text{facil}}} + U(1 - u)\delta(t - t^{\text{sp}}), \tag{4}$$

where x, y, and z represent the fractions of neurotransmitters in the recovered (available), active, and inactive state (refractory or recovering), respectively. u corresponds to the fraction of available resources (x) used in each presynaptic spike becoming active. In Eq. (1), τ_{rec} is the recovery time for inactive neurotransmitters. In Eq. (2), τ_{ina} is the decay time for neurotransmitters from active to inactive state. In Eqs. (1) and (2), the Dirac delta function moves the fraction xu of neurotransmitter from the recovery state to the active one at the instant which a spike is considered in the model, namely t^{sp}. We consider that when $t = t^{\text{sp}}$, the delta Dirac function can be approximated by the Kronecker delta so that $\delta(t - t^{\text{sp}}) = 1$, otherwise $\delta(t - t^{\text{sp}}) = 0$. In Eq. (3), the amount of recovering neurotransmitters depends on the inactivation and recovery process. In Eq. (4), τ_{fac} is the time for the synapses to return from the facilitation regime. As τ_{fac} approximates to zero, less facilitation is exhibited in the model. U describes how u value increases and is associated with the percentage of available neurotransmitters which are released due to each spike. In this work, we fixed the parameters τ_{rec} = 800 ms, τ_{ina} = 3 ms, and τ_{fac} = 1000 ms [22]. Thus, we studied the parameters U and t^{sp}, where t^{sp} is related to the mean spike frequency F and mean period $T = 1/F$. We consider the initial condition $x = 1$ and $y = z = u = 0$, which corresponds to a synapse with no recent activity and neurotransmitters totally recovered.

Fig. 1(a) shows a schematic representation of the neurotransmitters in the synapse by means of the variables x, y, and z. When a spike is considered in the model, the fraction of recovered neurotransmitters x can be released in the synaptic cleft, assuming an active state y that effectively will generate a current in the postsynaptic neuron. After the activation, these fraction of neurotransmitters are inactivated staying in the z variable until be in the recovered state x again and restart the cycle.

3. Results

Definitions and notations

The variables x, y, and u are continuous in time when the evolution is considered between two sequential spike events, from the time immediately after a spike event until the last time immediately before the next spike event. The variable z is continuous all the time. We define $t' = t - t^{\text{sp}} = 0$ to represent the time immediately after the spike of the neuron where $\delta(t') = 1$. Fig. 1(b) shows the time evolution of the
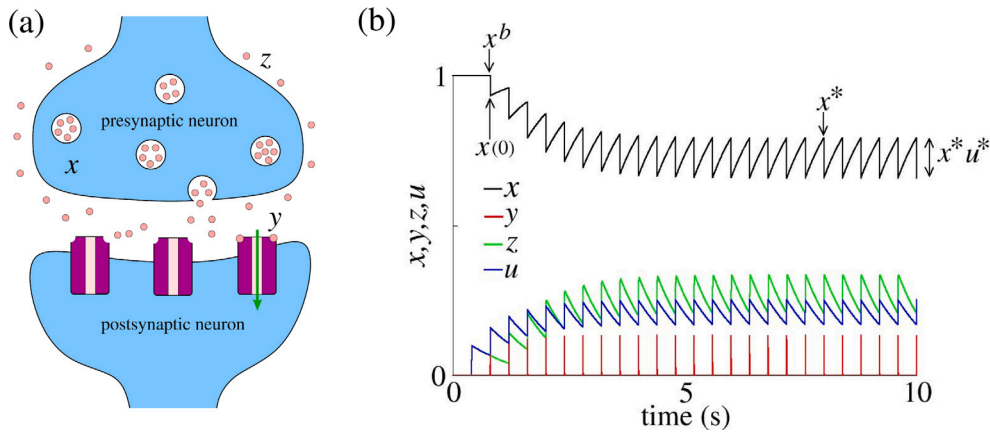
Fig. 1. (a) Schematic representation of the neurotransmitter states in a synaptic connection. x, y, and z stand for recovered, active, and inactive neurotransmitters, respectively. (b) Variable evolution x, y, z, u overtime for the facilitation regime. x^b and $x(0)$ stand by the x variable immediately before and after the spike event, respectively. x^* stands the fixed point of x after the transient time immediately before the spike event in the periodic spike regime. $x^* u^*$ represents the amount of neurotransmitters removed from the recovered state x and added to active state y. The same notation is used to identify the values of the variables before and after the spike event, as well as the fixed point after the transient. In Figure (b), we fixed $U = 0.1$ and $F = 2.5$ Hz.

variables, where x^b corresponds to the value of x immediately before the spike (t^{sp}). $x(0)$ and x^a represent both the value of x immediately after a spike event ($t = t^{sp}$), with the notation $x(0)$ being used to handle the variables describing the evolution of the system of ODEs. Such notation is extended for other variables, y, z, and u. In this way, it is possible to relate the variable value before and after each spike to be considered in all variables that are also described by the Eqs. (1)–(4) by

$$x(0) = x^a = x^b - u^b x^b, \tag{5}$$
$$y(0) = y^a = y^b + u^b x^b, \tag{6}$$
$$z(0) = z^a = z^b, \tag{7}$$
$$u(0) = u^a = u^b + U(1 - u^b). \tag{8}$$

Note that Eqs. (5)–(8) for the left equalities represent the time "t^{sp}" immediately after the first spike occurs in the presynaptic neuron. In the right equality of Eqs. (5)–(8), in a more general case, these equations relate the variable values immediately before (^{b}) and after (^{a}) the spike events.

Analytical approximation

To improve our understanding of the synaptic model, we search for an analytical approximation. We seek a solution between two sequential spike events for the set of differential Eqs. (1)–(4). We note that a general solution for $y(t')$ and $u(t')$ is independent of the other variables, resulting in

$$y(t') = y(0)e^{-\frac{t'}{\tau_{\text{ina}}}} \quad \text{and} \quad u(t') = u(0)e^{-\frac{t'}{\tau_{\text{fac}}}}, \tag{9}$$

where $t' \in [0, t^{sp}]$, t^{sp} being the time interval terminating just before the next spike happens. These solutions can be obtained just by integrating directly Eqs. (2) and (4). As can be observed, given a certain initial condition of these two variables, $y(0)$ and $u(0)$, the time evolution of y and u is determined until just before the next spike event. Since we have a solution for $y(t')$ and $z(t')$, it is possible to find an approximation for the solution of Eq. (3), replacing the solutions of Eq. (9) in Eq. (3), which result in

$$z(t') = \left[z(0) + y(0)(1 - e^{-t'/\tau_{\text{ina}}})\right] e^{-t'/\tau_{\text{rec}}}. \tag{10}$$

Considering now the solution of Eq. (10) into Eq. (1), similarly we have done to find the $z(t')$, we determine the solution of Eq. (1) as

$$x(t') = x(0) - z(0)(e^{-t'/\tau_{\text{rec}}} - 1)$$

$$-y(0)\left[(e^{-t'/\tau_{\text{rec}}} - 1) - \frac{\tau_{\text{ina}}}{\tau_{\text{rec}} + \tau_{\text{ina}}} e^{-t'\left(\frac{1}{\tau_{\text{ina}}} + \frac{1}{\tau_{\text{rec}}}\right)}\right]. \tag{11}$$

Taking into account Eqs. (5)–(8) and the following definitions

$$A(t') = e^{-t'/\tau_{\text{ina}}}, \quad B(t') = e^{-t'/\tau_{\text{rec}}}, \quad C(t') = e^{-t'/\tau_{\text{fac}}}, \tag{12}$$

and

$$E(t') = B(t')\left[1 - \frac{\tau_{\text{ina}}}{\tau_{\text{rec}} + \tau_{\text{ina}}} A(t')\right], \tag{13}$$

we can write Eqs. (9), (10), and (11) as

$$x(t') = (x^b + y^b) - z^b[B(t') - 1] - (y^b + x^b u^b)E(t'), \tag{14}$$
$$y(t') = (y^b + u^b x^b)A(t'), \tag{15}$$
$$z(t') = \left\{z^b + (y^b + x^b u^b)\left[1 - A(t')\right]\right\} B(t'), \tag{16}$$
$$u(t') = \left[u^b + U(1 - u^b)\right] C(t'). \tag{17}$$

Note that Eqs. (12) and (13) are considered to make the solutions in Eqs. (8)–(10) more compact, the result is presented in Eqs. (14)–(17). This compact solution describes the variable values for t' times after a spike. In other words, given a spike event that occurs when the variables are equal to x^b, y^b, z^b, u^b, the variable values after t' are equal to $x(t')$, $y(t')$, $z(t')$, and $u(t')$.

Synaptic map model - Periodic regime

For periodic presynaptic spikes with a certain frequency F, the period between two spikes is given by $T = 1/F$ and we set $t' = t - t^{sp} = T$. The map is constructed by relating the value of the variables at the time $t' = T$ (immediately before the second spike)

$$(x_{n+1}, y_{n+1}, z_{n+1}, u_{n+1}) = (x, y, z, u), \tag{18}$$

with those of the variables at the time $t' = 0$ (immediately before the first spike)

$$(x_n, y_n, z_n, u_n) = (x^b, y^b, z^b, u^b). \tag{19}$$

Thus, this map relates the value of the variables immediately before two consecutive spikes. This is important because such values determine the changes in synaptic variables as well as the fraction of active neurotransmitters.

From Eqs. (14)–(17), we obtain the map for the synapse

$$x_{n+1} = (x_n + y_n) - z_n[B(T) - 1] - (y_n + x_n u_n)E(T), \tag{20}$$
$$y_{n+1} = (y_n + x_n u_n)A(T), \tag{21}$$
$$z_{n+1} = \left\{z_n + (y_n + x_n u_n)\left[1 - A(T)\right]\right\} B(T), \tag{22}$$

$$u_{n+1} = [u_n + U(1 - u_n)]\, C(T). \tag{23}$$

Fixed point solutions

For periodic spikes, after a certain transient time, the equilibrium point represented by x^*, y^*, z^* and u^* is achieved. The equilibrium point is obtained by solving the system

$$(x_{n+1}, y_{n+1}, \ldots) = (x_n, y_n, \ldots) = (x^*, y^*, \ldots), \tag{24}$$

which lead us to

$$x^* = 1 - y^* - z^*, \tag{25}$$

$$y^* = [y^* + x^* u^*] A(T), \tag{26}$$

$$z^* = \{z^* + [y^* + x^* u^*][1 - A(T)]\} B(T), \tag{27}$$

$$u^* = [u^* + U(1 - u^*)]C(T), \tag{28}$$

and finally

$$x^* = \frac{A(T)[1 + B(T)] + B(T) - 1}{D(T)}, \tag{29}$$

$$y^* = \frac{A(T)[B(T) - 1]}{D(T)} u^*, \tag{30}$$

$$z^* = \frac{B(T)[A(T) - 1]}{D(T)} u^*, \tag{31}$$

$$u^* = \frac{U C(T)}{1 + [U - 1]C(T)}, \tag{32}$$

where

$$D(T) = A(T)B(T)[2u^* - 1] + [A(T) + B(T)][1 - u^*] - 1, \tag{33}$$

and A, B and C are defined in Eqs. (12), for $t' = T$.

Approximation for low frequency

In the numerical simulation, we considered a small value of the time for inactivation given by $\tau_{\text{ina}} = 3$ ms. Such value generates a fast decay in the y variable, so that we can approximate y_n to zero in Eqs. (20), (21), and (22). In this case, we also can approximate $A(T)$ to 0 since we can neglect $A(T)$ for the inactivation time constant $\tau_{\text{ina}} = 3$ ms and low frequencies, rewriting the map of Eqs. (20)–(22) as

$$x_{n+1} = x_n - z_n[B(T) - 1] - x_n u_n B(T), \tag{34}$$

$$y_{n+1} = 0, \tag{35}$$

$$z_{n+1} = \{z_n + [x_n u_n]\} B(T), \tag{36}$$

$$u_{n+1} = [u_n + U(1 - u_n)]C(T). \tag{37}$$

Noticing that $B(T)$ and $C(T)$ for the time constants $\tau_{\text{rec}} = 800$ ms and $\tau_{\text{fac}} = 1000$ ms have typically a far from zero value for low frequencies and we can rewrite the fixed points as

$$x^* = \frac{B(T) - 1}{D}, \tag{38}$$

$$y^* = 0, \tag{39}$$

$$z^* = \frac{-B(T)}{D(T)} u^*, \tag{40}$$

$$u^* = \frac{U C(T)}{1 + [U - 1]C(T)}, \tag{41}$$

where

$$D(T) = B(T)[1 - u^*] - 1. \tag{42}$$

Numerical analysis

By a numerical approach, we study the synaptic regimes as the function of the constant spike frequency F and the amount of neurotransmitter released associated with the parameter U. The range of U is taken in the interval from the minimal ($U_{\min} = 0$) to the maximal fraction ($U_{\max} = 1$) of neurotransmitters that can become active due to a spike in a certain time. Values higher than 1 are related to an amount of neurotransmitters higher than the available in the synapse. There is no negative fraction of neurotransmitters. The range for the frequency is taken in an appropriate interval where the regimes, maximal, and equilibrium values change considerably for the combinations of U and F, for the parameters considered in our study [22].

To classify the synaptic regimes we considered the evolution of y because it represents the effective fraction of neurotransmitters that is transmitted from the presynaptic to the postsynaptic neuron [22]. To mentioning, the synaptic current induced in the postsynaptic neuron is given by

$$I_{\text{syn}}(t') = (V_{\text{pre}}^{\text{rev}} - V_{\text{post}})g_c\, y(t'), \tag{43}$$

where $V_{\text{pre}}^{\text{rev}}$ is the synaptic reversal potential associated with the presynaptic neuron type (excitatory or inhibitory), V_{post} is the potential of the postsynaptic neuron, g_c is the maximal synaptic conductance in the chemical synapse, and $y(t')$ is the fraction of active neurotransmitters released by the presynaptic neuron [7,22,48]. This quantity described by the model is the effective amount of neurotransmitters released due to each spike event, which in the considered case has amplitude

$$y(t') = x^b u^b A(t') = y^a A(t'). \tag{44}$$

This value represents the fraction of neurotransmitters in the active state that will arrive in the receptors. x^b and u^b are the values of x and u variables immediately before the spike, respectively, y^a is the value of y immediately after the spike. This quantity is the effective amount of active neurotransmitters released due to each spike event. Such values depend on the initial conditions and history of the synaptic activity.

Synaptic regimes - Periodic

Fig. 2(a)–(c) show examples of the three different regimes for periodic spikes, namely (a) facilitation, (b) biphasic, and (c) depression. The red line represents the fraction of active neurotransmitters, $y(t)$, while the green points, y^a, represent the maximal value of y due to each spike which describes the value of y immediately after the spike event. Based on this value, we define the three synaptic regimes previously mentioned. Facilitation corresponds to the synaptic regime where the value of active neurotransmitters only increases due to each spike or remains with an equal intensity after the transient period. Depression is the case where the value of active neurotransmitters only decreases due to each spike or remains at the same value after a transient time. Biphasic is associated with the synaptic regime where there is an increase and decrease in the value of active neurotransmitters. $y_{\max}$ represents the maximal value of y over time, while y_{fin} indicates the final amplitudes of y after the transient time for periodic spikes. In Fig. 2(a)–(c), we considered $F = 2.5$ Hz, Fig. (a) $U = 0.1$ for facilitation, Fig. (b) $U = 0.4$ for biphasic, and Fig. (c) $U = 0.8$ for the depression regime. The mentioned parameters are indicated in Fig. 2(d) by white square, circle, and triangle, respectively. Fig. 2(d) displays the synaptic regimes in the parameter space of the fraction of neurotransmitters released and the periodic spike frequency, U and F, respectively. As can be seen in the figure, the synaptic regimes are dependent on the parameters. The facilitation regime is found for the lowest frequency or smallest probabilities of neurotransmitter release, or both conditions. Depression is mainly found in the highest values of neurotransmitter release. A biphasic regime appears between the two previously cited regimes. In the map, we can identify the different regimes taken into account if some conditions are satisfied. In the facilitation regime, the
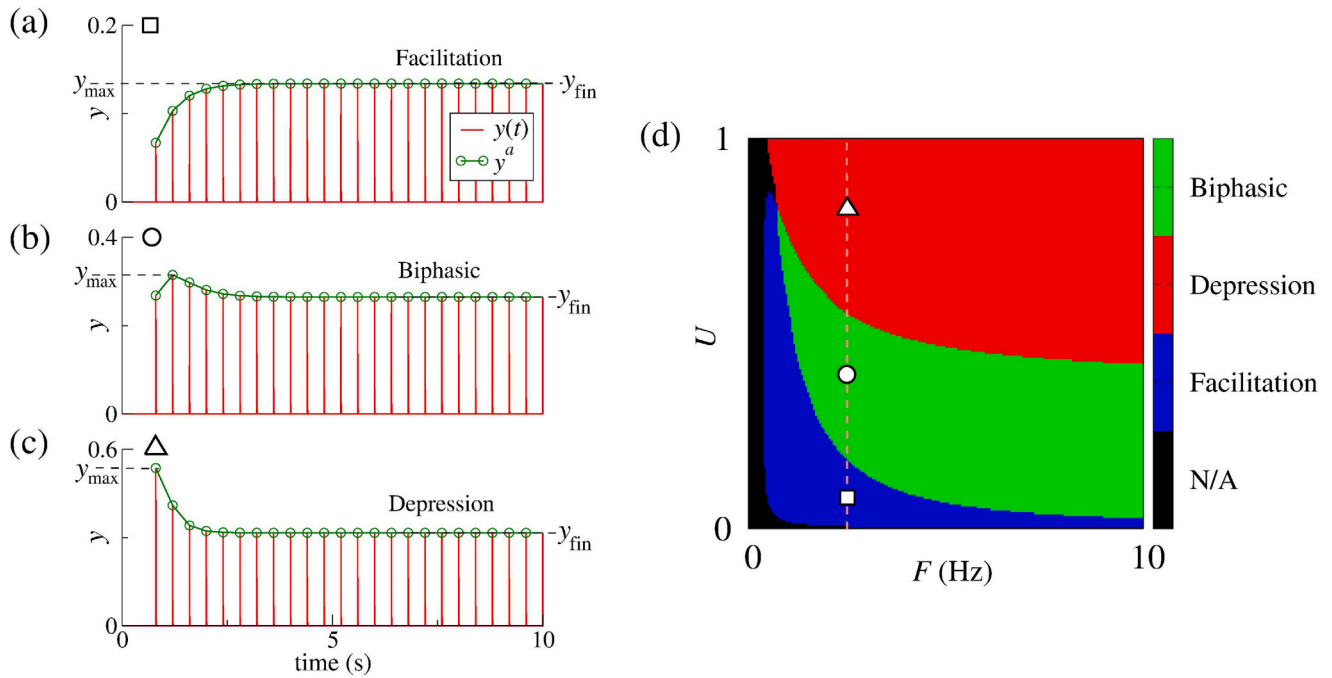
Fig. 2. (a–c) Dynamics of the active neurotransmitters in the synapse for three different regimes, (a) facilitation, (b) biphasic, and (c) depression. Red lines show the dynamics of active neurotransmitters represented by the y variable, and the green line with circles represents the y amplitude immediately after the spike event, $y^a = y(0)$. In Figs. (a–c), we consider $F = 2.5$ Hz, (a) $U = 0.1$ for facilitation, (b) $U = 0.4$ for biphasic, and (c) $U = 0.8$ for depression regime. In Figs. (a–c), the maximal value of y overtime is identified as y_{max} while the final amplitude of y is represented by y_{fin}. (d) Regimes found in the dynamics synapses: facilitation, depression and biphasic. The facilitation and depression regimes are identified by means of Eqs. (45) and (46). If both conditions of Eqs. (45) and (46) are satisfied over time we identified the biphasic regime. The parameters U and F considered in Figs. (a–c) are indicated in Fig. (a). (For interpretation of the references to colour in this figure legend, the reader is referred to the web version of this article.)

amplitude of y variable will always increase or be equal to the final value x^*u^* if

$$x_n(T)u_n(T) \leq x_{n+1}(T)u_{n+1}(T), \tag{45}$$

for $n > 1$ with fixed U and T, otherwise, for the depression regime, the amplitude of y variable will reduce or be equal to the final value x^*u^*, if the condition

$$x_n(T)u_n(T) \geq x_{n+1}(T)u_{n+1}(T) \tag{46}$$

is satisfied for $n > 1$ with fixed U and T. If the Eqs. (45) and (46) are satisfied in different iterations for $n > 1$, and fixed T and U values, the synapse exhibits a biphasic regime. If the fraction of neurotransmitter released or frequency assumes values very near to zero, the value of active neurotransmitters behaves as a linear dynamics where there is no change on this value (very small frequencies) or very close to zero (U close to zero), consequently, it is not possible to identify the regime in the parameter space. We identify such dynamics as "N/A" (not applicable) since the considered methodology does not identify such regimes, once conditions in Eqs. (45) and (46) become close to equalities. The different regimes obtained in our simulation, namely facilitation, depression, and biphasic, qualitatively agree with experimental [22] and reconstructions of synaptic dynamics in silico [49].

Final fraction of active neurotransmitters - Periodic

Fig. 3(a) shows the time evolution of the variables given by the model described by the ODE taking into account only the time immediately before the spike event. The figure also exhibits the value of y immediately after considering the spike event (y^a) due to its importance in synaptic communication. The values of the fixed points of the map are determined by Eqs. (38)–(41). The black dashed lines indicate the calculated fixed points x^*, y^*, z^*, and u^*, as well as the final value of y immediately after the spike event, y_{fin}. The value of y_{fin} is given by

$$y_{fin} = x^*u^*. \tag{47}$$

Such values do not depend on the historic and initial conditions of the synapse. Note that for this model the initial condition $x(0)$, $y(0)$, $z(0)$, and $u(0)$ must satisfy $x(0) + y(0) + z(0) = 1$ and $u(0) = [0,1]$.

As it can be observed, the calculated fixed points agree with the evolution of the dynamics by Eqs. (1)–(4), as well as the synaptic map model. Fig. 3(b) and (c) show the maximal and final value of y, where y_{fin} is obtained after the transient time. In Fig. 3(b), the maximal value corresponds to the highest value of y due to its entire time evolution given the initial condition of the synapse in the rest. The maximal values in the temporal series are found for the highest U and F values. However, these highest values of y might appear only briefly, cases observed in depression and biphasic regimes. For facilitation, the maximal y values correspond to y_{fin} and are exhibited after the transient time. As can be seen in Fig. 3(c), the final values of y do not appear for large frequencies, but there is a range of frequencies where y_{fin} is higher. For such a range of frequency, the higher values of U leads to higher y_{fin}.

Maximal fraction of active neurotransmitters - Periodic

We study the maximal fraction of active neurotransmitters for a synapse initially on the rest. Fig. 4 displays the number of map iterations to obtain the maximal value of y from a synapse initially in the rest. We iterate the map and plot the number of iterations to arrive at the maximal fraction of active neurotransmitters. Fig. 4(a)–(d) shows the y^a dynamics for (a) depression, (b) and (c) biphasic, and (d) facilitation regime, identifying the y_{max} by a blue square. For depression, the maximal value occurs for $n = 1$ while for biphasic regime occurs for $n \geq 2$. Fig. 4(e) shows the n value to find y_{max} in the synaptic map considering the initial condition of the synapse on the rest state. The n value to obtain the y_{max} varies on the parameter space $F \times U$.

To analytically determine the maximal values for the three synaptic regimes, we consider the following initial condition of the synapse on
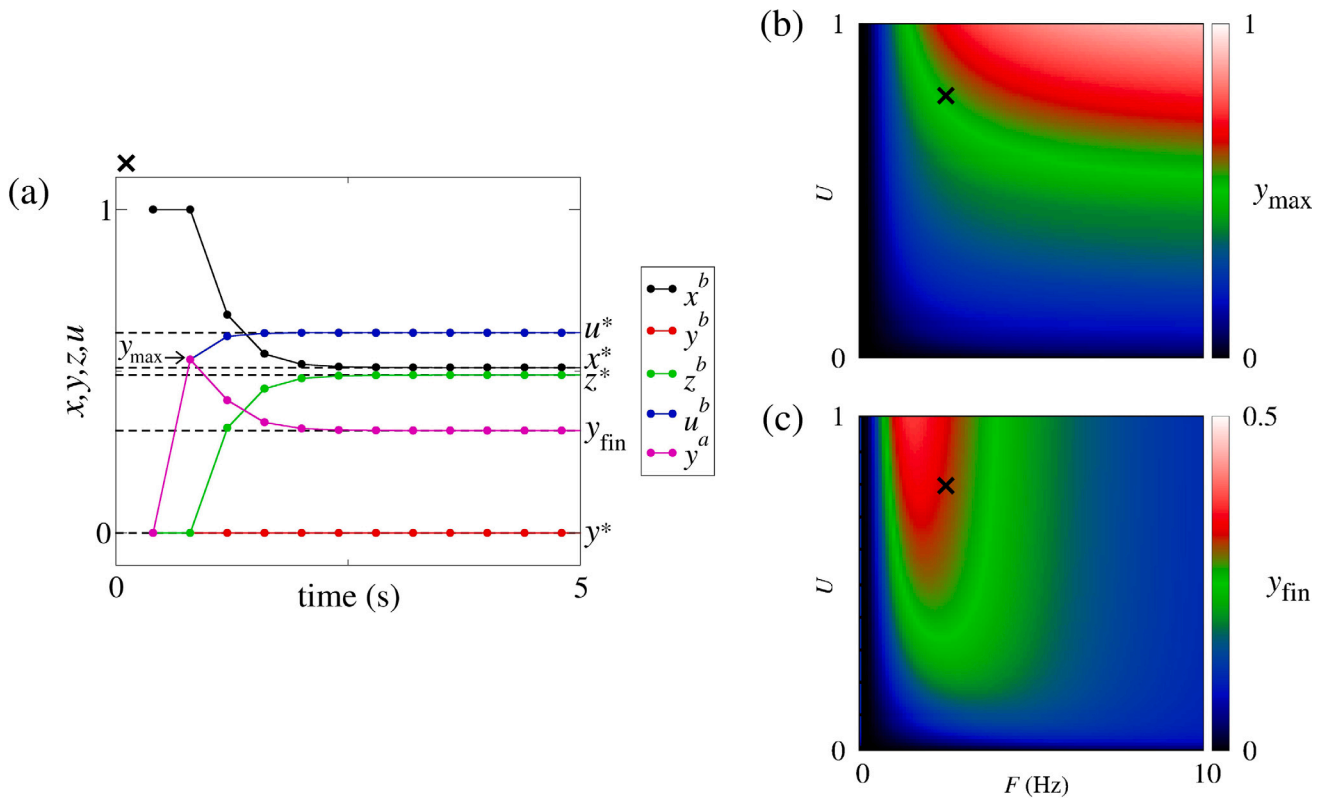
Fig. 3. (a) Time evolution of the variable values immediately before considering the spike event on the synaptic model described by the ODE (x^b, y^b, z^b, u^b). As the y variable is responsible for generating the current in the postsynaptic neuron, the value of y immediately after considering the spike event (y^a) and $y_{\max}$, are also indicated in the figure. The black dashed lines represent the calculated equilibrium points, x^*, y^*, z^*, and u^* of the discrete map, as well as the final value y_{fin}. The parameters $U = 0.8$ and $F = 2.5$ Hz are indicated in figures (b) and (c) by a black X. (b) Maximal y values in the parameter space $U \times F$. $y_{\max}$ is obtained as the maximal value of y in the entire temporal evolution of the model. (c) y_{fin} in the equilibrium point, which is the y amplitude immediately after each spike past the transient time.

rest,

$$x_0 = 1, \qquad y_0 = 0, \qquad z_0 = 0, \qquad \text{and} \qquad u_0 = 0. \tag{48}$$

These values represent the state variables immediately before the first spike. One map iteration takes them to the states immediately before the second spike, given by

$$x_1 = 1, \qquad y_1 = 0, \qquad z_1 = 0, \qquad \text{and} \qquad u_1 = UC(T). \tag{49}$$

For the depression regime shown in Fig. 4(a), the maximal value of y is given by Eq. (15) for $t' = 0$, and therefore equal to

$$y_{\max} = x_1 u_1 = UC(T). \tag{50}$$

For the biphasic regime showed in Fig. 4(b,c), the maximal y value is also provided by Eq. (15) for $t' = 0$, however depending on the parameters that maximal is only reached after a certain number of spikes. So,

$$y_{\max} = x_i u_i, \tag{51}$$

where i representing the number of spikes applied to the initial condition at rest can assume values equal to 2, 3, 4, …. Abusing the notation and dropping the argument (T) of $A(T)$, $B(T)$, and $C(T)$, for simplicity, the variable states immediately before the second spike is given by

$$x_2 = 1 - UBC, \qquad y_2 = 0, \qquad z_2 = UBC, \tag{52}$$
$$\text{and} \quad u_1 = UC^2 + UC(1 - UC). \tag{53}$$

Inputting these values into Eq. (15) provides the potential maximal value after 2 spikes of the neuron ($i = 2$) given by

$$y_{\max} = x_2 u_2 = U\{2C - UC^2[1 + 2B - BC]\}.$$

This maximal value for $i = 2$ is predominant in the parameter space $F \times U$ for the biphasic regime. The larger the value of i, the smaller the area in the parameter space, showing that it is less likely to be observed. Notice that to calculate the maximal values analytically, the larger the value of i the larger the degree of the polynomial associated with the solution sought. So, we only calculate maximal values up to $i = 2$.

Finally, for the facilitation regime shown in Fig. 4(d), the maximal value of y is asymptotically increasing towards the equilibrium point and can be calculated by using the values from the equilibrium points in Eqs. (38) and (41) into Eqs. (14) and (17), and then plugging these values into Eq. (15) for $t' = 0$. Keeping in mind that x^* and u^* are the equilibrium values for x and u, for the facilitation regime we have

$$y_{\max} = x^* u^* = y_{\text{fin}}. \tag{54}$$

For F higher than 10 Hz, the synaptic regimes, n and the maximal values of active neurotransmitters have just a small shift in the parameter space for the constant parameters considered. However, as F increases, the fraction of active neurotransmitters in the equilibrium decreases.

Mean synaptic map model - Poisson

In this section, we consider non-periodic spike times given by a homogeneous Poissonian process to generate the time of spikes t^{sp}.
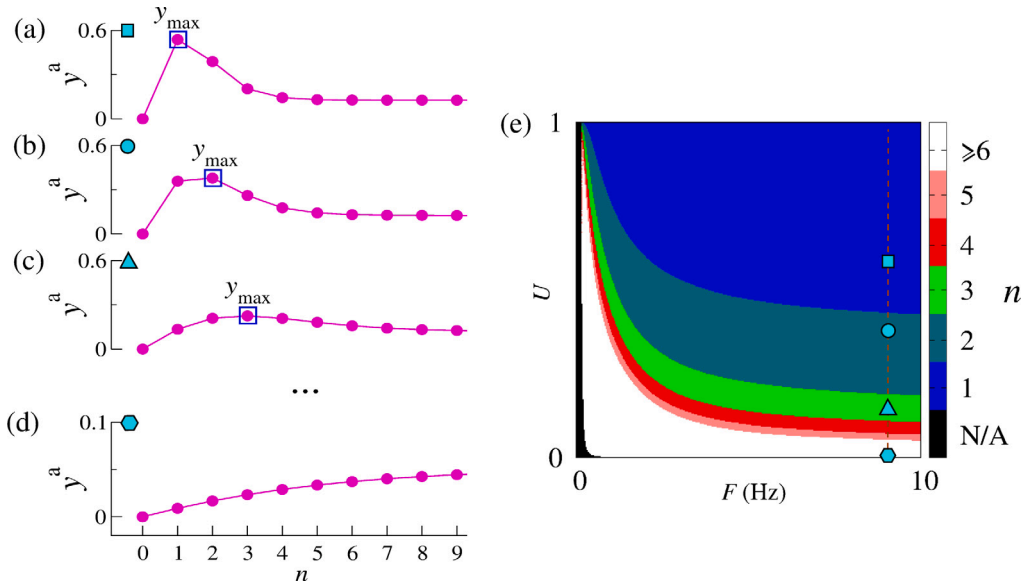
Fig. 4. y variable after the spike (y^a) for different values of the parameter of U identifying the maximal value (y_{max}). In Fig. (a–d), we fix $F = 9$ Hz, (a) $U = 0.6$, (b) $U = 0.4$, (c) $U = 0.15$ and (d) $U = 0.01$. Fig. (e) shows the number of iterations to find the maximal value of y from the rest state of the synapse. (For interpretation of the references to colour in this figure legend, the reader is referred to the web version of this article.)

Different from the periodic case, the time interval T between two spikes is not constant but rather is described by a Poisson process and thus assumes different values for each iteration. Namely, for $N+1$ iterations, we have $T_0, T_1, T_2, \ldots, T_N$, where N is considered as a large integer value. Just showing the iteration for these time intervals for the y variable described by Eq. (21), we have

$$y_1(T_0) = y_0 A(T_0) + x_0 u_0 A(T_0), \tag{55}$$

$$y_2(T_1) = y_1 A(T_1) + x_1 u_1 A(T_1), \tag{56}$$

$$y_3(T_2) = y_2 A(T_2) + x_2 u_2 A(T_2), \tag{57}$$

$$\cdots = \cdots + \cdots \tag{58}$$

$$y_{N+1}(T_N) = y_N A(T_N) + x_N u_N A(T_N). \tag{59}$$

Considering the sum of all the terms in the equations and dividing by $N + 1$ to obtain a temporal average, we find

$$\frac{1}{N+1} \sum_{n=0}^{N} y_{n+1}(T_n) = \frac{1}{N+1} \sum_{n=0}^{N} \left[y_n A(T_n) + x_n u_n A(T_n) \right].$$

Identifying the mean values by

$$\overline{y_{n+1}} = \frac{1}{N+1} \sum_{n=0}^{N} y_{n+1}(T_n), \tag{60}$$

$$\overline{y_n A(T_n)} = \frac{1}{N+1} \sum_{n=0}^{N} y_n A(T_n), \tag{61}$$

$$\overline{x_n u_n A(T_n)} = \frac{1}{N+1} \sum_{n=0}^{N} x_n u_n A(T_n), \tag{62}$$

we can write the expression of the temporal average for the y variable as

$$\overline{y_{n+1}} = \overline{y_n A(T_n)} + \overline{x_n u_n A(T_n)}. \tag{63}$$

Taking into account that the product of the mean is equal to the mean of products, we can rewrite the last expression as

$$\overline{y_{n+1}} = (\overline{y_n} + \overline{x_n}\ \overline{u_n})\overline{A(T_n)}. \tag{64}$$

To determine the value of $\overline{A(T_n)}$, we consider the power series expansion for exponential function in the case that $T_n \ll \tau_{fac}$, obtaining the approximation

$$\overline{A(T_n)} = \frac{1}{N+1} \sum_{n=0}^{N} \sum_{m=0}^{\infty} \frac{1}{m!} \left(\frac{-T_n}{\tau_{fac}} \right)^m$$

$$= \frac{1}{N+1} \sum_{m=0}^{\infty} \frac{(-1)^m}{m!} \left(\frac{T_0^m + T_1^m + T_2^m + \cdots T_N^m}{\tau_{fac}^m} \right)$$

$$\approx \sum_{m=0}^{\infty} \frac{1}{m!} \left(\frac{-T}{\tau_{fac}} \right)^m = A(T). \tag{65}$$

Using the same calculations for the other map variables in Eqs. (20), (22), and (23), for a homogeneous Poisson process, we obtain the map evolution of the temporal average given by

$$\overline{x_{n+1}} = (\overline{x_n} + \overline{y_n}) - \overline{z_n}[B(T) - 1] - (\overline{y_n} + \overline{x_n}\ \overline{u_n})E(T), \tag{66}$$

$$\overline{y_{n+1}} = (\overline{y_n} + \overline{x_n}\ \overline{u_n})A(T), \tag{67}$$

$$\overline{z_{n+1}} = \left\{ \overline{z_n} + (\overline{y_n} + \overline{x_n}\ \overline{u_n})[1 - A(T)] \right\} B(T), \tag{68}$$

$$\overline{u_{n+1}} = [\overline{u_n} + U(1 - \overline{u_n})]C(T). \tag{69}$$

The temporal averaged map for the Poissonian presynaptic spikes exhibits the same evolution as the synaptic map for presynaptic neurons spiking periodically, since the equations are the same. These equations for the temporal averaged map admit a solution for the equilibrium point if

$$\overline{x_{n+1}} = \overline{x_n} = x^*, \tag{70}$$

$$\overline{y_{n+1}} = \overline{y_n} = y^*, \tag{71}$$

$$\overline{z_{n+1}} = \overline{z_n} = z^*, \tag{72}$$

$$\overline{u_{n+1}} = \overline{u_n} = u^*. \tag{73}$$

Since Eqs. (20)–(23) are the same as Eqs. (66)–(69), the equilibrium points of the periodic stimulus are the same for the mean values in Poissonian stimulus. The mean value of the active neurotransmitters for Poisson spikes remains the same as the final value of active neurotransmitters for the periodic spikes. In other words, the time average value of xu immediately before spikes for both the Poissonian and periodic spikes tends to product x^*u^*. Based on that result, our analysis suggests that the average behaviour of a synapse forced by Poissonian spikes is determined by the dynamics of synapses driven by periodic spikes.

Distinguishing from the periodic case, when the spikes follow a Poisson process it is not possible to determine the synaptic regimes since the fraction of active neurotransmitters released oscillates in time with higher and lower values than the periodic spikes. For this reason, the maximal values of y can be significantly higher for the Poisson spikes than for the periodic ones.

4. Conclusions

In this paper, we study short-term plasticity considering the model proposed by Tsodyks et al. [22]. We focus our analysis on the synaptic regimes facilitation, depression, and biphasic that emerge as a function of the frequency and fraction of released neurotransmitters. Depression regime is mainly dependent on the percentage of released neurotransmitters, while facilitation is observed for low frequencies or small amounts of neurotransmitter release, or for both cases. The biphasic regime is found between the facilitation and depression, being a combination of both regimes. This model presents both depression and facilitation mechanisms. Some simplified versions provide only one of such regimes. It takes in account the emergence of both regimes depending on the synaptic parameters and firing frequency.

Our main result was to obtain an approximated solution for the set of differential equations and derive a map where the synaptic dynamics can be understood in terms of the time intervals between the spike events. From this map, we determined analytically the equilibrium points for periodic spiking regimes, allowing for the determination of the asymptotic values of active neurotransmitters as a function of the frequency, the probability release of neurotransmitters, and the time constants. We also determined the expected maximal and asymptotic values for the three synaptic regimes. We observe that the highest value of active neurotransmitters occurs by a brief time period from the rest regime in the depression and biphasic regime, while for the facilitation regime, the maximal values are the asymptotic ones.

Furthermore, we obtain a temporal average map when the time intervals between spikes follow a Poisson distribution and show that the equilibrium point for such a configuration is the same as found for the periodic spikes. This result suggests that the time average dynamics of a stochastic driven synapse emulating presynaptic spikes by a complex neural network is regulated by the periodically driven synapses.

To better understand the dynamic response of our synaptic model in the presence of presynaptic neurons, we consider that these neurons spike following a Poisson distribution. This hypothesis is often done in the literature. However, other more general stochastic dynamics could be considered as a way to emulate the spiking regime of neurons connected in a network. A stochastic description would, however, be an approximation. Ideally, the spiking regime of presynaptic neurons should be determined either experimentally or by a neural network of realistic neural models connected under a synaptic model that could be ours.

One practical implication of our results is the analytical description of the synaptic dynamics, which can provide insights into how neurons communicate and synchronize. Our map has analytical solutions, then very large neuronal networks, considering our realistic synaptic model, can be considered to make simulations in computational neuroscience, artificial neural networks, and neuroengineering. It is possible to obtain analytical solutions of the synaptic dynamics, thus speeding up simulations of very large multi-synaptic networks [50]. In addition, since the alternation of the fraction of neurotransmitters released is observed in some neuronal disorders [51,52], developing drugs capable of restoring the normal fraction on the synapses can be a potential strategy to relive symptoms or treat brain diseases. Advances in the research on such topic can be based on the theoretical results showed in the present work.

We believe that our results can allow other neuroscientist to construct neuronal networks with a biologically relevant synaptic model that can be analytically solved. In the future, we plan to extend the results for correlated spikes, burst patterns [53], inhomogeneous spike times [54] as well as spike sequences induced by spontaneous network activities [55].

CRediT authorship contribution statement

Paulo R. Protachevicz: Conceptualization, Data curation, Formal analysis, Investigation, Methodology, Software, Visualization, Writing – original draft, Writing – review & editing, Funding acquisition, Validation. **Antonio M. Batista:** Conceptualization, Visualization, Writing – original draft, Writing – review & editing, Methodology. **Iberê L. Caldas:** Conceptualization, Funding acquisition, Methodology, Supervision, Visualization, Writing – original draft, Writing – review & editing. **Murilo S. Baptista:** Conceptualization, Formal analysis, Investigation, Supervision, Validation, Visualization, Writing – original draft, Writing – review & editing.

Declaration of competing interest

The authors declare that they have no known competing financial interests or personal relationships that could have appeared to influence the work reported in this paper.

Data availability

Data will be made available on request.

References

[1] Di Maio V, Santillo S. Ventriglia f synaptic dendritic activity modulates the single synaptic event. Cogn Neurodyn 2021;15(2):279–97.

[2] Pereda AE. Electrical synapses and their functional interactions with chemical synapses. Nat Rev Neurosci 2014;15:250–63.

[3] Connors BW, Long MA. Electrical synapses in the mammalian brain. Annu Rev Neurosci 2004;27(1):393–418.

[4] Caire MJ, Reddy V, Varacallo M. Physiology, synapse. In: StatPearls. Treasure Island (FL): StatPearls Publishing; 2022.

[5] Bear MF, Connors BW, Paradiso MA, Michael A. Neuroscience: exploring the brain. 4th ed.. Jones and Bartlett Publisher, Inc.; 2020.

[6] Suszkiw JB. Synaptic transmission. In: Sperelakis N, editor. Cell physiology source book. 4th ed.. Elsevier; 2012, p. 563–78.

[7] Gerstner W, Kistler WM, Naud R, Paninski L. Neuronal dynamics: from single neurons to networks and models of cognition and beyond. Cambridge University Press; 2014.

[8] Roth A, van Rossum MCW. Modeling synapses. In: Schutter Erik De, editor. Computational modeling methods for neuroscientists. Cambridge, MA: MIT Press Scholarship Online; 2009.

[9] Sterrat D, Graham B, Gillies A, Willshaw D. The synapses. principles of computational modelling in neuroscience. Cambridge University Press; 2012.

[10] Tauffer L, Kumar A. Short-term synaptic plasticity makes neurons sensitive to the distribution of presynaptic population firing rates. eNeuro 2021;8(2):0297.

[11] Roberts PD. Synaptic dynamics: Overview. In: Jaeger D, Jung R, editors. Encyclopedia of computational neuroscience. New York: Springer; 2014.

[12] Citri A, Malenka RC. Synaptic plasticity: Multiple forms, functions, and mechanisms. Neuropsychopharmacology 2008;33:18–41.

[13] Deperrois N, Graupner M. Short-term depression and long-term plasticity together tune sensitive range of synaptic plasticity. PLoS Comput Biol 2020;16(9):e1008265.

[14] Kemp A, Manahan-Vaughan D. Hippocampal long-term depression and long-term potentiation encode different aspects of novelty acquisition. PNAS 2004;101(21):8192–7.

[15] Bliss TVP, Cooke SF. Long-term potentiation and long-term depression: a clinical perspective. Clinics. 2011;66:3–17.

[16] MacLeod KM, Horiuchi TK, Carr CE. A role for short-term synaptic facilitation and depression in the processing of intensity information in the auditory brain stem. J Neurophysiol 2007;97:2863–74.

[17] Cho S, Li G-L, von Gersdorff H. Recovery from short-term depression and facilitation is ultrafast and Ca^{+2} dependent at auditory hair cell synapses. J Neurosci Res 2011;31(15):5582–692.

[18] Howell RD, Pugh JD. Biphasic modulation of parallel fibre synaptic transmission by co-activation of presynaptic $GABA_A$ and $GABA_B$ receptors in mice. J Physiol 2016;594(13):3651–66, 1.

[19] Buonomano DV. Decoding temporal information: A model based on short-term synaptic plasticity. J Neurosci Res 2000;20(3):1129–41.

[20] Abbott LF, W.G. Regehr. Synaptic computation. Nature 2004;431:796–803.

[21] Deng P-Y, Klyachko VA. The diverse function of short-term plasticity components in synaptic computation. Commun Integr Biol 2011;2(5):543–8.

[22] Tsodyks M, Uziel A, Markram H. Synchrony generation in recurrent networks with frequency-dependent synapses. J Neurosci Res 2000;20:1–5.

[23] Citri A, Malenka RC. Synaptic plasticity: Multiple forms, functions, and mechanisms. Neuropsychopharmacol Rep 2008;33:18–41.

[24] Rotman Z, Deng P-Y, Klyachko VA. Short-term plasticity optimizes synaptic information transmission. J Neurosci Res 2011;31(41):148000-14809.

[25] Cortes JM, Desroches M, Rodrigues S, Veltz R, Muñoz MA, Sejnowski TJ. Short-term synaptic plasticity in the deterministic Tsodyks–Markram model leads to unpredictable networks dynamics. Proc Natl Acad Sci USA 2013;110(41):16610–5.

[26] Markram H, Wang Y, Tsodyks M. Differential signaling via the same axon of neocortical pyramidal neurons. Proc Natl Acad Sci USA 1998;95(9):5323–8.

[27] Fortune ES, Rose GJ. Short-term synaptic plasticity as a temporal filter. Trends Neurosci 2001;24(7):381–5.

[28] Barroso-Flores J, Herrera-Valdez MA, Galarraga E, Bargas J. Models of short-term synaptic plasticity. Adv Exp Med Biol 2017;1015:41–57, Springer International Publishing AG.

[29] Blitz DM, Foster KA, Regehr WG. Short-term synaptic plasticity: a comparison of two synapses. Vol. 5, Nature Publishing Group; 2004, p. 630–40.

[30] Jackman SL, Regehr WG. The mechanisms and functions of synaptic facilitation. Neuron 2017;94(3):447–64.

[31] Barak O, Tsodyks M. Persistent activity in neural networks with dynamic synapses. PLOS Comput Biol 2007;3(2):e35.

[32] Mondal Y, Pena RFO, Rotshein HG. Temporal filters in response to presynaptic spike trains: interplay of cellular, synaptic and short-term plasticity time scales. J Comput Neurosci 2022;50:395–429.

[33] Kass RE, Ventura V. A spike-train probability model. Neural Comput 2001;13(8):1713–20.

[34] Deger M, Cardanobile S, Helias M, Rotter S. The Poisson process with dead time captures important statistical features of neural activities. BMC Neurosci 2009;10:P110.

[35] Simen P, Balci F, deSouza L, Cohen JD, Holmes P. A model of interval timing by neural integration. J Neurosci Res 2011;31(25):9238–53.

[36] Burkitt AN. A review of the integrate-and-fire neuron model: I. Homogeneous synaptic input. Biol Cybernet 2006;95:1–19.

[37] Burkitt AN. A review of the integrate-and-fire neuron model: II. Inhomogeneous synaptic input and network properties. Biol Cybernet 2006;95:97–112.

[38] Cinlar E. Introduction to stochastic processes. Courier Corporation; 2013.

[39] Gabbiani F, Cox SJ. Mathematics for neuroscientist. Academic Press, Elsevier; 2010.

[40] Ladenbauer J, McKenzie S, English DF, Hagens O, Ostojic S. Inferring and validating mechanistic model of neural microcircuits based on spike-train data. Nature Commun 2019;10:4933.

[41] Pena RFO, Zaks MA, Roque AC. Dynamics of spontaneous activity in random networks with multiple neuron subtypes and synaptic noise. J Comput Neurosci 2018;45:1–28.

[42] Droste F, Lindner B. Up-down-like background spiking can enhance neural information transmission. eNeuro 2017;4(6):0282-17.2017.

[43] Snyder DL, Miller MI. Poisson process. In: Snyder DL, Miller MI, editors. Random point processes in time and space. Springer texts in electrical engineering, New York, NY: Springer; 1991, p. 1–40.

[44] Goris RLT, Movshon JA, Simoncelli EP. Partitioning neuronal variability. Nature Neurosci 2014;17(6):858-565.

[45] Mazzoni A, Broccard FD, Garcia-Perez E, Bonifazi P, Ruaro ME, Torre V. On the dynamics of the spontaneous activity in neuronal networks. PLos One 2007;2(5):e439.

[46] Tsodyks MV, Markram H. The neural code between neocortical pyramidal neurons depends on neurotransmitters release probability. Proc Natl Acad Sci 1997;94:719–23.

[47] Bertolotti E, Burioni R, di Volo M, Vezzani A. Synchronization and long-time memory in neural networks with inhibitory hubs and synaptic plasticity. Phys Rev E 2017;95:012308.

[48] Protachevicz PR, Borges FS, Lameu EL, Ji P, Iarosz KC, Kihara AH, Caldas IL, Szezech Jr JD, Baptista MS, Macau EEN, Antonopoulos CG, Batista AM, Kurths J. Bistable firing pattern in a neural network model front. Comput Neurosci 2020;13(19).

[49] Markram H, Muller E, Ramaswamy S, Reimann MW, Abdellah M, Sanchez CA, Ailamaki A, Alonso-Nanclares L, Antille N, Arsever S, Kahou GA, Berger TK, Bilgili A, Buncic N, Chalimourda A, Chindemi G, Courcol JD, Delalondre F, Delattre V, Druckmann S, Dumusc R, Dynes J, Eilemann S, Gal E, Gevaert ME, Ghobril JP, Gidon A, Graham JW, Gupta A, Haenel V, Hay E, Heinis T, Hernando JB, Hines M, Kanari L, Keller D, Kenyon J, Khazen G, Kim Y, King JG, Kisvarday Z, Kumbhar P, Lasserre S, Le Bé JV, Magalhães BR, Merchán-Pérez A, Meystre J, Morrice BR, Muller J, Muñoz-Céspedes A, Muralidhar S, Muthurasa K, Nachbaur D, Newton TH, Nolte M, Ovcharenko A, Palacios J, Pastor L, Perin R, Ranjan R, Riachi I, Rodríguez JR, Riquelme JL, Rössert C, Sfyrakis K, Shi Y, Shillcock JC, Silberberg G, Silva R, Tauheed F, Telefont M, Toledo-Rodriguez M, Tränkler T, Van Geit W, Díaz JV, Walker R, Wang Y, Zaninetta SM, DeFelipe J, Hill SL, Segev I, Schürmann F. Reconstruction and simulation of neocortical microcircuitry. Cell 2015;163:456–92.

[50] Fauth M, Wörgotter F, Tetzlaff C. The formation of multi-synaptic connections by the interaction of synaptic and structural plasticity and their functional consequences. PLoS Comput Biol 2015;11(1):e1004031.

[51] Sheffler ZM, Reddy V, Pillarisetty LS. Physiological, neurotransmitters. Tresure Island; 2023.

[52] Teleanu RI, Niculescu AG, Roza E, Vladâcenco O, Grumezescu AM, Teleanu DM. Neurotransmitters-key factors in neurological and neurodegenerative disorders of the central nervous system. Int J Mol Sci 2022;23(11):5954.

[53] Protachevicz PR, Borges FS, Iarosz KC, Baptista MS, Lameu EL, Hansen M, Caldas IL, Szezech Jr JD, Batista AM, Kurths J. Bistable firing patterns in a neural network model. Front Physiol 2020;11.

[54] Amarasingham A, Chen TL, Geman S, Harrison MT, Sheinberg DL. Spike count reliability and the Poisson hypothesis. J Neurosci 2006;26(3):801–9.

[55] Borges FS, Protachevicz PR, Pena RFO, Lameu EL, Higa GSV, Kihara AH, Matias FS, Antonopoulos CG, de Pasquale R, Roque AC, Iarosz KC, Ji P, Batista AM. Self-sustained activity of low firing rate in balanced networks. Physica A 2020;537:122671.